JMEPEG (2016) 25:179–187
DOI: 10.1007/s11665-015-1828-z


1059-9495/$19.00

# Influence of Processing Parameters on Grain Size Evolution of a Forged Superalloy

*L.A. Reyes, P. Páramo, A. Salas Zamarripa, M. de la Garza, and M.P. Guerrero-Mata*

*(Submitted June 24, 2015; in revised form October 23, 2015; published online December 17, 2015)*

**The microstructure evolution of nickel-based superalloys has a great influence on the mechanical behavior during service conditions. Microstructure modification and the effect of process variables such as forging temperature, die-speed, and tool heating were evaluated after hot die forging of a heat-resistant nickel-based alloy. Forging sequences in a temperature range from 1253 to 1323 K were considered through experimental trials. An Avrami model was applied using finite element data to evaluate the average grain size and recrystallization at different evolution zones. It was observed that sequential forging at final temperatures below 1273 K provided greater grain refinement through time-dependent recrystallization phenomena. This investigation was aim to explore the influence of forging parameters on grain size evolution in order to design a fully homogenous and refined microstructure after hot die forging.**

**Keywords** forging, grain size, modeling and simulation, recrystallization, superalloys

## 1. Introduction

Inconel 718 superalloy is a Ni-Fe-Cr alloy that combines high-temperature strength up to 700 °C with high resistance to oxidation and corrosion. This superalloy is commonly used in components for power generation and aircraft applications (Ref 1). Inconel 718 is reinforced by solid solution and precipitation of second phases, generally by different heat treatments. The hardening mechanism is mainly contributed by precipitation of $\gamma'$ $Ni_3Al$ (cubic or spherical shape) and $\gamma''$ $Ni_3Nb$ phase (Ref 2). The metastable $\gamma''$ phase transforms to stable $Ni_3Nb$-$\delta$ phase during exposure at temperatures above 923 K, leading to degradation of mechanical properties (Ref 3). However, $\delta$ phase present in Inconel 718 plays an important role in the control of grain size during hot working (Ref 4). Forging of Inconel 718 is performed at temperatures varying around 1273 K at which some dispersed precipitates of $\delta$ phase limit grain growth (Ref 5). Below 1213 K, the $\gamma'$ and $\gamma''$ precipitates harden the material, leading to excessive compression stresses during hot forging (Ref 6).

Deformation at high temperature usually triggers a marked transformation of microstructure called recrystallization. This phenomenon can be defined as the generation of new high-angle, mobile grain boundaries, and their subsequent migration driven by stored energy in the form of dislocation. When it happens during deformation, it is called dynamic recrystallization (DRX) and when it occurs after deformation, it is termed static recrystallization (SRX). In some cases, DRX may initiate through nucleation but may not proceed to completion during deformation. In these cases, the recrystallization is completed after deformation by the growth of dynamically nucleated grains. This is known as metadynamic recrystallization (MDRX) (Ref 7). Metals with low or medium levels of stacking fault energy such as copper and nickel undergo DRX while metals with high stacking fault energy undergoes dynamic recovery (Ref 8). The final grain size commonly depends on softening mechanisms due to dynamic recovery and recrystallization phenomena. These mechanisms in turn depend on the initial microstructure, chemical composition, and forming conditions (Ref 9).

The mechanical properties of Inconel 718 are greatly influenced by the microstructure evolution. Controlling the grain size under narrow process windows is of great importance due to its influence on the mechanical strength of manufactured components (Ref 10). Extensive research studies have been focus mainly on grain size evolution with temperature, strain, and strain rate of deformation on lab scale samples where deformation conditions have been carefully controlled (Ref 3). However, non-isothermal trials can give a better insight on grain size evolution during forging process. In recent years, some investigations on the hot deformation behaviors of nickel-based superalloys have been carried out. Chen (Ref 11) studied the dynamic recrystallization behavior of a nickel-based superalloy by hot compression tests. Based on the conventional DRX kinetics model, the volume fractions of DRX were estimated. Lin et al. (Ref 12) studied the high-temperature deformation behavior of a Ni-based superalloy by compression tests over practical ranges of temperature and strain rate. Based on the experimental data, phenomenological constitutive models were established to describe the work hardening-dynamic recovery and dynamic flow softening behavior of the studied superalloy. Also, Lin et al. (Ref 13) studied the hot tensile deformation behaviors and fracture characteristics of a typical Ni-based superalloy and found that the DRX characteristics appear under relatively high deformation temperatures (1283 and 1313 K).

**L.A. Reyes** and **A. Salas Zamarripa**, Facultad de Ingeniería Mecánica y Eléctrica, Universidad Autónoma de Nuevo León, San Nicolás de los Garza, NL, Mexico and Centro de Innovación, Investigación y Desarrollo en Ingeniería y Tecnología, Universidad Autónoma de Nuevo León, San Nicolás de los Garza, NL, Mexico; and **P. Páramo, M. de la Garza,** and **M.P. Guerrero-Mata,** Facultad de Ingeniería Mecánica y Eléctrica, Universidad Autónoma de Nuevo León, San Nicolás de los Garza, NL, Mexico. Contact e-mail: larturoreyes@gmail.com.

In a multi-step forging process, the work-piece is reheated in a furnace between each stroke, generating new homogeneous microstructures as a new deformation sequence starts. The metadynamic recrystallization and static recrystallization occur during forging processes (Ref 14) owing to the almost full completion of recrystallization mechanism between two passes (Ref 15). The recrystallization phenomenon is not only an important softening mechanism, but also an effective method to refine the coarse grain size and reduce the hot deformation resistance. The grain size has to be fine and homogenous to ensure the required performance is achieved in service conditions (Ref 16). Prediction of microstructure is essential when attempting to control mechanical properties and deformation process of final product. Different models have been proposed to predict microstructural changes during recrystallization. The Avrami equation is often used to evaluate the softening fractions induced by DRX, MDRX, and SRX. This empirical mathematical model was widely used to model the flow behavior and microstructure for industrial applications (Ref 17). Avrami models have been used to predict the softening fractions induced by recrystallization phenomena of steels (Ref 18) and nickel-based superalloys (Ref 19). In this work, experimental trials were developed to evaluate the microstructure evolution of Inconel 718 superalloy under hot forging conditions. Recrystallization and grain growth were modeled using an Avrami model coupled with a commercial finite element platform Deform V11 3D. Different recrystallization phenomena were considered to take place during sequential forging operations (either at one step or two steps) in the forging range of 1323 to 1253 K. The aim of this investigation is to explore the influence of forging parameters on grain refinement in order to generate a fully refine microstructure.

## 2. Experimental Procedure

The material used in this investigation is a commercial nickel-based superalloy; the chemical composition is shown in Table 1. A cylindrical preform was used for the experimental trials; eight specimens were sectioned and machined to a final dimension of 100 mm × 150 mm for diameter and height, respectively. An industrial hydraulic press with a maximum force of 2500 Tons and maximum velocity of 20 mm/s (apparent strain rate 0.13 $S^{-1}$) was used to perform forging process; tooling contact surfaces were heated at 523 K for top region and 673 K for the bottom part. The grain size of Inconel 718 depends highly on the presence of δ phase of which the solution temperature is around 1313 K (Ref 5). Since fine grain size was preferred, the forging temperature was selected to be near solvus temperature of δ phase. Forging temperature was varied from 1323 to 1253 K considering single- and two-step forging operations as shown in Table 2 (1 to 4 single-step forged; 5 to 8 two-step forged). One- or two-step forging processes are regularly employed for superalloy disk forging operations.

**Table 1 Chemical composition of Inconel 718 nickel-based superalloy studied (wt.%)**

| Ni | Cr | Nb + Ta | Mo | Ti | Al | Co | C | Fe |
|---|---|---|---|---|---|---|---|---|
| 53.79 | 17.96 | 5.42 | 2.88 | 1.01 | 0.51 | 0.34 | 0.026 | Bal. |

Prior to forging operation, grain size measurements were conducted according to ASTM E112 (Ref 20) at different locations as illustrated in Fig. 1. Grain size was measured at three different zones (top, center and bottom) and 4 angular locations (0°, 90°, 180°, and 270°), see Table 3. Presence of duplex grains (different distributions of grain size) in all the regions of analysis was observed.

After forging, the grain size was measured and an effective grain size was determined by the relation;

$$d = f_d(d_1 f_1 + d_2 f_2) \quad \text{(Eq 1)}$$

where $f_1$ y $f_2$ are fractions of fine grain and un-recrystallized grain, respectively, $d_1$ is the fine grain size, and $d_2$ is the thick grain size (Ref 21). The distribution of fine grains in duplex microstructure is represented by $f_d$. If fine grains are distributed in collar form around un-recrystallized grains, $f_d$ takes a value of 0.5, otherwise the value is 1.

## 3. Numerical Modeling

A numerical model was developed assuming a 2D symmetric simplification of a cylinder with diameter of 100 mm and height of 150 mm to reduce the computation cost. Mechanical properties were acquired from previous investigation (Ref 22). Friction and heat transfer conditions on the die-sample interface have a significant effect on flow behavior and required forging loads. It has been shown that a shear stress friction factor generates better results compared to coulomb friction coefficient due to high contact stresses (Ref 23). In this model, a shear friction factor $m$ of 0.3 and an interfacial coefficient of 1.3114 W/mm$^2$/K were used (Ref 24). Air convection for cooling was considered and a heat transfer coefficient of 0.02 W/mm$^2$ °C was selected.

**Table 2 Experimental test conditions of specimens forged at single- and two-step operations**

| Test number | Initial temperature for 1st forging step, K | Strain for 1st forging step | Initial temperature for 2nd forging step, K | Strain for 2nd forging step |
|---|---|---|---|---|
| 1 | 1323 | 0.73 | … | … |
| 2 | 1293 | 0.73 | … | … |
| 3 | 1273 | 0.73 | … | … |
| 4 | 1253 | 0.73 | … | … |
| 5 | 1313 | 0.50 | 1293 | 0.23 |
| 6 | 1293 | 0.50 | 1273 | 0.23 |
| 7 | 1293 | 0.50 | 1253 | 0.23 |
| 8 | 1273 | 0.50 | 1253 | 0.23 |

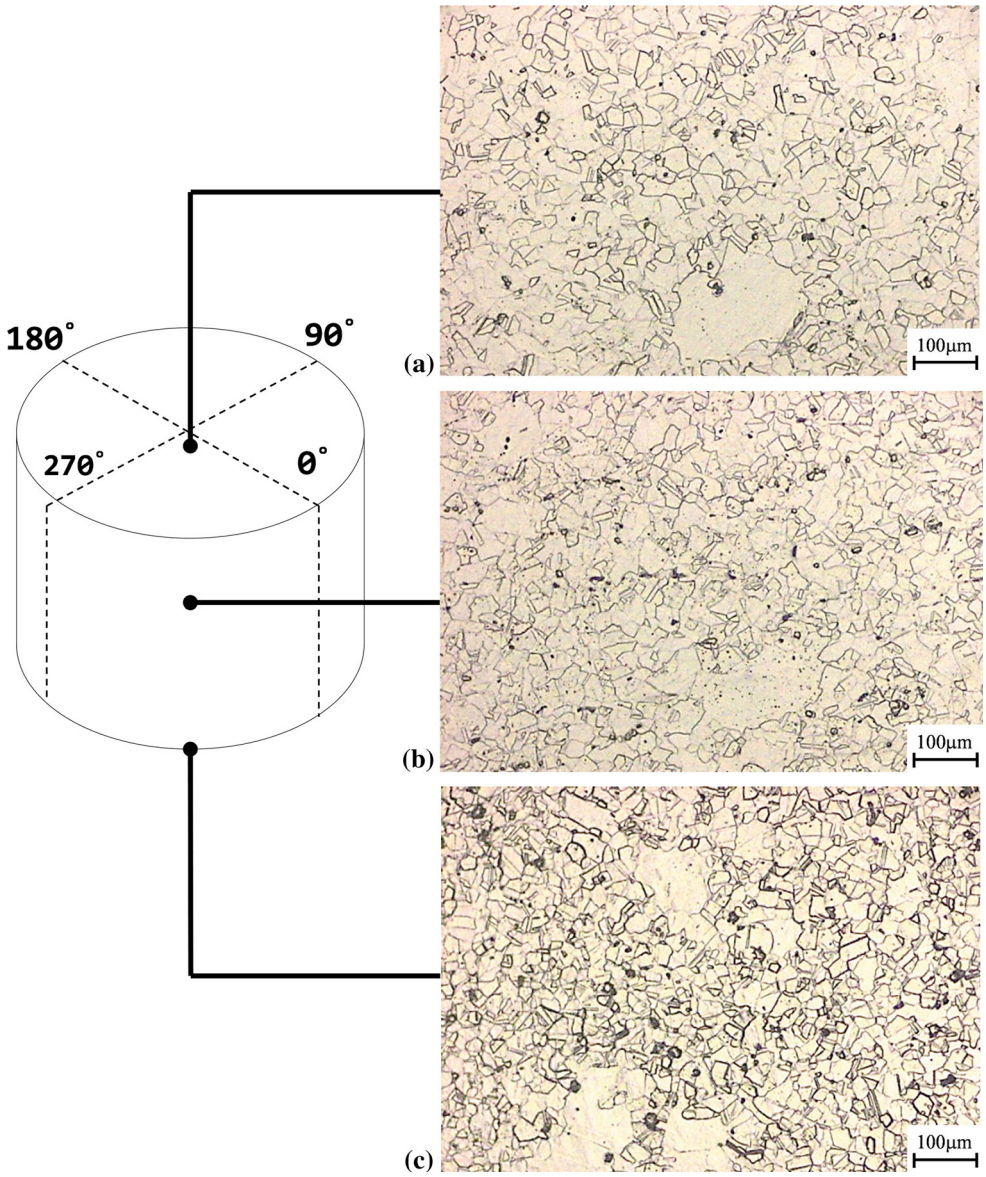


**Fig. 1** Specimen for experimental trials and initial grain size measurements at different zones and angular locations (0°, 90°, 180°, and 270°); (a) Top surface, (b) Center, and (c) Bottom surface

**Table 3 Experimental results of initial grain size measurements at different angular location for specimens to be compressed at temperatures from 1323 to 1253 K**

| Test number | Grain size measurement at different angles, μm | | | | Average Grain size | Larger Grain size |
|---|---|---|---|---|---|---|
| | 0° | 90° | 180° | 270° | | |
| 1 | 35 | 41 | 34 | 104 | 53.5 | 151 |
| 2 | 63 | 48 | 41 | 53 | 51.2 | 213 |
| 3 | 22 | 71 | 75 | 72 | 60.0 | 302 |
| 4 | 52 | 40 | 82 | 61 | 58.7 | 213 |
| 5 | 74 | 67 | 40 | 104 | 71.2 | 213 |
| 6 | 35 | 62 | 43 | 47 | 46.7 | 213 |
| 7 | 77 | 47 | 103 | 51 | 69.5 | 254 |
| 8 | 42 | 51 | 45 | 41 | 44.7 | 179 |

**Table 4 Parameters of Avrami model for the nickel-based superalloy studied (Ref 27)**

| Description | Equation | Parameter |
|---|---|---|
| DRX kinetics | $X_{DRX} = 1 - \exp\left[-\beta_d \left(\frac{t}{\varepsilon_{0.5}}\right)^{k_d}\right]$ | $\beta_d = 0.693$; $k_d = 2$ |
| DRX grain size | $d_{drx} = a_8 d_0^{h_8} \varepsilon^{n_8} \dot{\varepsilon}^{m_8} \exp\left(\frac{Q_8}{RT}\right)$ | $a_8 = 4.85e10$; $n_8 = -0.41$; $m_8 = -0.028$; $Q_8 = -240{,}000$ |
| MDRX kinetics | $X_{MDRX} = 1 - \exp\left[-\beta_m \left(\frac{t}{t_{0.5}}\right)^{k_m}\right]$ | $\beta_m = 0.693$; $k_m = 1$ |
| MDRX grain size | $d_{mdrx} = a_7 d_0^{h_7} \varepsilon^{n_7} \dot{\varepsilon}^{m_7} \exp\left(\frac{Q_7}{RT}\right)$ | $a_7 = 4.85e10$; $n_7 = -0.41$; $m_7 = -0.028$; $Q_7 = -240{,}000$ |
| Grain growth | $d_g = \left[d_0^m + a_9 t \exp\left(\frac{-Q_9}{RT}\right)\right]^{1/m}$ | $a_9 = 1.58e16$; $Q_9 = 390{,}753$; $m = 2$ |

## 4. Microstructure Models

### 4.1 Avrami Model

During hot forging different microstructural changes can occur, the recrystallization model known as Avrami model is often used to evaluate the softening fractions induced by dynamic recrystallization and metadynamic recrystallization. This is the classical method to compute average grain sizes based on thermomechanical and metallurgical parameters (Ref 25). The general form of the Avrami equation for recrystallized fraction as a function of time is described by the equation:

$$X = 1 - \exp(-k\,t^n), \qquad \text{(Eq 2)}$$

In Eq 2, the term $k$ is typically a function of the rate at which the nuclei are formed and the rate at which the grains grow. The exponent $n$ is usually known as Avrami exponent. For DRX, Avrami equation typically is represented by the expression:

$$X = 1 - \exp\left[-\ln 2 \left(\frac{\varepsilon - \varepsilon_c}{\varepsilon_{0.5} - \varepsilon_c}\right)^n\right]. \qquad \text{(Eq 3)}$$

In this equation, $\varepsilon$ is the applied strain; $\varepsilon_{0.5}$ is the required strain at specific temperature and deformation rate to recrystallized half of initial structure during deformation; $\varepsilon_c$ is the critical deformation to span a nucleus and begin recrystallization. Usually, the critical strain for the initiation of DRX can be expressed as a function of peak strain ($\varepsilon_p$). For the studied superalloy, the critical strain can be estimated as $\varepsilon_c = 0.80\varepsilon_p$. Once the deformation degree exceeds the critical strain, DRX takes place (Ref 26). This is because, while the growth of the first nuclei produces softening locally, the remaining material continues to work harden. For the DRX of nickel-based superalloys the Avrami exponent takes values around 2 to 3 (Ref 9).

During MDRX further recrystallization occurs without the addition of any strain, the recrystallization fraction is primarily a function of the time. MDRX time $t_{0.5}$ is defined as the time after deformation in which half of microstructure had been recrystallized. The equation for MDRX it expressed by:

$$X = 1 - \exp\left[-\ln 2 \left(\frac{t}{t_{0.5}}\right)^n\right], \qquad \text{(Eq 4)}$$

where the time $t_{0.5}$ depends on strain grade, deformation velocity, and dwell time after forging. Typically, MDRX grains are coarser than dynamically recrystallized grains. When the MDRX process is complete, any extended hold at elevated temperatures causes the grains to grow statically. Grain growth occurs either immediately following hot working or during heating prior to hot working. A general expression that describes the static grain growth is expressed by Eq 5.

$$d_g = \left[d_0^m + at\,\exp\left(\frac{-Q}{RT}\right)^{1/m}\right]. \qquad \text{(Eq 5)}$$

In this expression, $a$ and $Q$ are constants, and $m$ is an exponent with value of 2 or 3. This equation also considers the initial grain size $d_0$, temperature $T$, and time $t$ as determining variables. In Table 4, Arrhenius and power laws are used into quantify the dependence of recrystallized grain size on process variables and the initial grain size $d_0$ of Inconel 718 superalloy. The parameters for the Avrami model used in this study were collected from previous investigations (Ref 27). These expressions were incorporated into the finite element program DEFORM V11 3D to determine the grain size after forging operation. An average grain size is considered according to the evaluation of initial grain size by the methodology presented in Fig. 1. In addition, a recrystallized fraction of 0.5 was defined for initial microstructure computations.

## 5. Results

The microstructure of Inconel 718 superalloy after hot deformation was affected by processing variables as shown in Fig. 2. Three zones are clearly distinguished for grain size distribution after forging; top, bottom, and central zone. The central zone was fully recrystallized with homogeneous distribution of grain size, while top and bottom regions were partially recrystallized. Base on previous microstructure evolution data, the experimental and simulated results will be focused on these three regions.

Refinement of grain size and increase of recrystallized fraction results after one-step forging as illustrated in Fig. 3. Fully recrystallized microstructure was observed for center zone of samples 1 and 2 forged at 1323 and 1293 K, respectively. Recrystallization is a phenomenon that consists in two stages; nucleation and growing on new grains. For this event to take place is necessary reach a critical dislocation density through the interface of nucleus and the surrounding material (Ref 28). Top and bottom regions present grain growth with partial recrystallization. However, due to insufficient flowing during deformation and heat transfer between tooling and experimental samples, these zones do not present significant grain refinement. Considering the Nb content of the nickel-based alloy studied, it is possible that forging at 1293 K do not present excessive grain growth due pinning effect of needle-like precipitates (Ref 5).

Abnormal grain growth was observed in samples single forged at 1273 and 1253 K. This abnormal grain growth

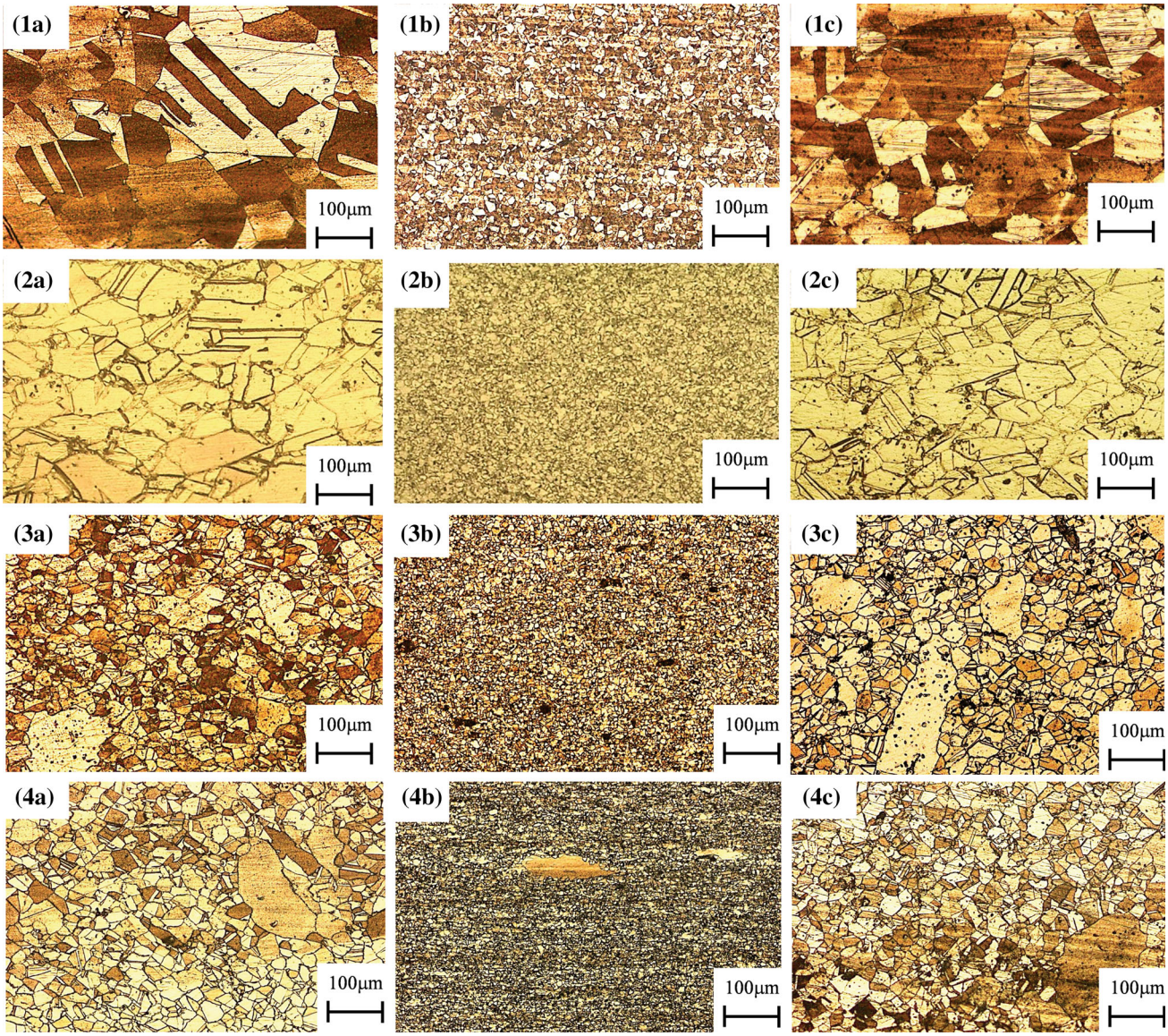


**Fig. 2** Image of macroetched grain (HCl-$C_2H_6O$-$HNO_3$) for one-step forging condition (Ref 3) at 1000 °C

occurred as a result of migration of interfaces with local high velocities (Ref 29). However, there are just a few studies related with secondary recrystallization of high-strength nickel superalloys (Ref 16). Figure 4 shows metallographic results of samples two-step forged in the range of 1313-1253 K. It was observed a fully recrystallized microstructure at the center of conditions 5 and 6 with a final forging temperature of 1293 and 1273 K, respectively. Comparing conditions 3 and 5 deformed at final temperature of 1293 K both conditions presented a fine grain size of 18 μm in the central region. The same similarity is observed for conditions 3 and 6 with a final forging temperature of 1273 K. An average grain size of 11 μm was obtained for both forging conditions either at one and two-step operations.

From numerical results, the effective strain and average grain size for sample 6 forged at 1293-1273 K is observed in Fig. 5. This forged condition has an average grain size of 11 μm in central region and an increase of recrystallized fraction after cooling, as seen in Fig. 6. The results from RX simulation and average grain size show good fit with the experimental data. Comparing samples forged at one and two sequences, second forging shows a greater influence of metadynamic recrystallization due to the time available during deforming cycles.

The relationship between recrystallized volume fraction and strain effective at forging (Ref 5) 1313-1293 K and (Ref 6) 1293-1273 K is shown in Fig. 7. For the samples studied DRX fraction presents a decrease for strain effective in the interval of 0.5-1.25, reaching a maximum in the central region of forged samples. The change of DRX fraction of two-step forged samples occurred due to the previous evolving RX fraction during first-step forging. In addition, the evolution of dynamically recrystallized grain size increased with increasing temperature.

At high effective strains, particularly values above 1.5, it was observed an opposite effect in RX phenomena presenting an increase in DRX fraction, while MDRX fraction decreases as reaching the central region. As the strain increases, the

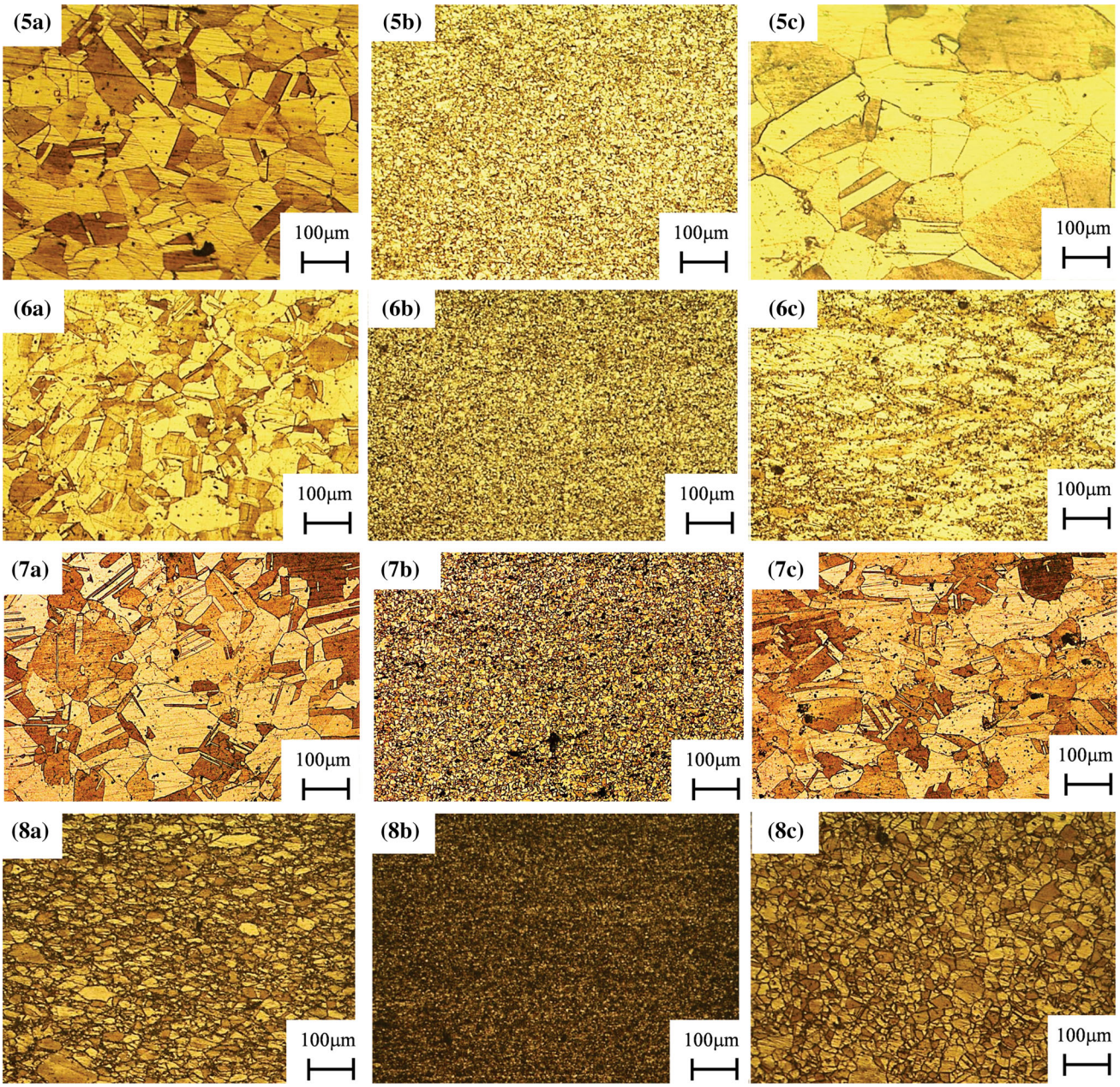


**Fig. 3** Micrographs at 100X (HCl-$C_2H_6O$-$HNO_3$) for one-step forging conditions; (1a) Top-1050 °C, (1b) Center-1050 °C, (1c) Bottom-1050 °C, (2a) Top-1020 °C, (2b) Center-1020 °C, (2c) Bottom-1020 °C, (3a) Top-1000 °C, (3b) Center-1000 °C, (3c) Bottom-1000 °C, (4a) Top-980 °C, (4b) Center-980 °C, and (4c) Bottom-980 °C

density of grains also increases, indicating ongoing nucleation during DRX. Average grain size at center location is affected by DRX developing a greater refinement in the second forging operation. A maximum in metadynamic fraction was observed at effective strain of 0.5. The MDRX fraction decrease as strain increase reaching the central zone where DRX is the principal recrystallization mechanism acting. MDRX of Inconel 718 is related to the growth of the preexisting dynamically recrystallized grains. This mechanism shows a high dependence in the initial grain size and degree of strain. It is possible that this phenomenon is related with unrecovered dislocation density accumulated in refined grains and its density increases with deformation. However, to gain full understanding of the recrystallization kinetics more information should be analyzed in detail, particularly regions subject to low strains and partial recrystallization. Under this condition, the strain energy is not sufficient to initiate dynamic recrystallization. Techniques such as transmission electron microscopy (TEM) and electron backscattered diffraction (EBSD) can provide grain boundary information for the deformed superalloy.

The resulting grain size for the forging trials studied is indicated in Fig. 8. Under the temperature of evaluation two domains of microstructure evolution were observed; at temperatures below 1293 K, the grain size is control by blocking of precipitate particles generating a fine grain size. At temperatures above 1293 K growth of grain size is observed either for one- and two-step forgings.

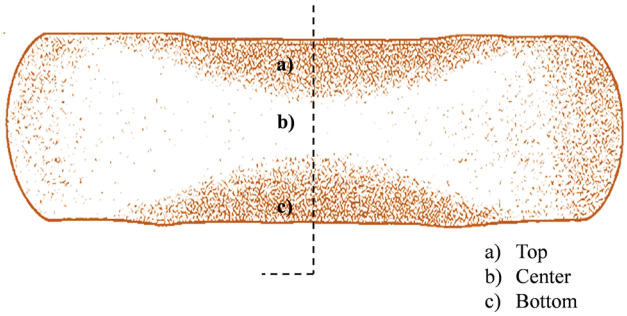


**Fig. 4** Micrographs at 100X ($HCl\text{-}C_2H_6O\text{-}HNO_3$) for two-step forging conditions; (5a) Top 1040-1020 °C, (5b) Center 1040-1020 °C, (5c) Bottom 1040-1020 °C, (6a) Top 1020-1000 °C, (6b) Center-1020-1000 °C, (6c) Bottom 1020-1000 °C, (7a) Top 1020-980 °C, (7b) Center 1020-980 °C, (7c) Bottom 1020-980 °C, (8a) Top 1000-980 °C, (8b) Center 1000-980 °C, and (8c) Bottom 1000-980 °C

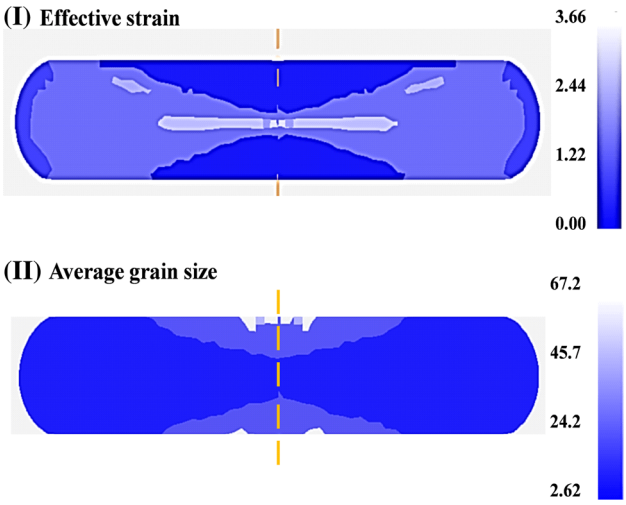


**Fig. 5** Numerical results of two-step forging condition (Ref 6) 1020-1000 °C. (a) Effective strain and (b) average grain size (μm)

The greatest divergence of grain size take place at regions of stagnant flow, particularly at sample 1 forged at 1323 K; see section (a) of Fig. 8. Under this condition, it is developed an accelerated grain growth during heating of samples previous to forging as shown in previous investigations (Ref 30). For an Inconel 718 superalloy with a contain of 5%Nb, an average grain size of 30 μm will growth until reaching a value of 100 μm after heating 30 min at 1313 K (Ref 31). Forging at two steps shows a grater refinement particularly for samples 7 and 8 forged at final temperature of 1273 and 1253 K, respectively. This refinement being depended on time is indicative of statistical necessity to wait that nucleation occurred and allow new regions with active nucleus growth (Ref 32). Top region presents partial recrystallization and high dependence on strain rate and grade of strain, and these variables in conjunction with temperature are the main factors for generation of nucleation sites.

In general, the validity and precision of numerical models will depend on inherent limitations of each particular model. The Avrami models take in account that the material store energy is uniformly distributed and the recrystallized phases will growth isotropically. Also, models are not sensible to

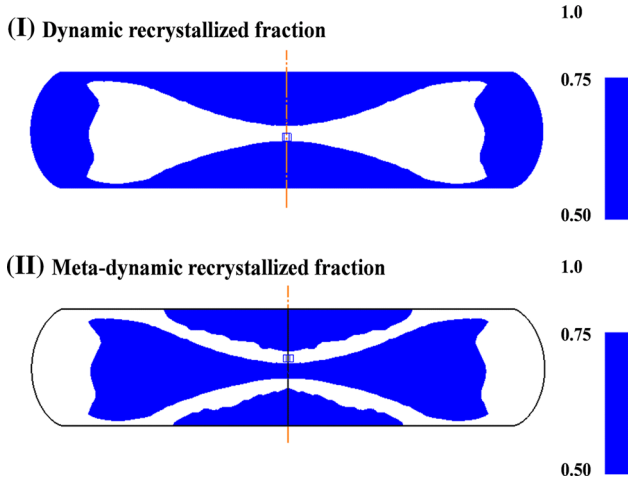


**Fig. 6** Numerical results of two-step forging condition (Ref 6) 1020-1000 °C. (a) Dynamic recrystallized fraction and (b) Metadynamic recrystallized fraction

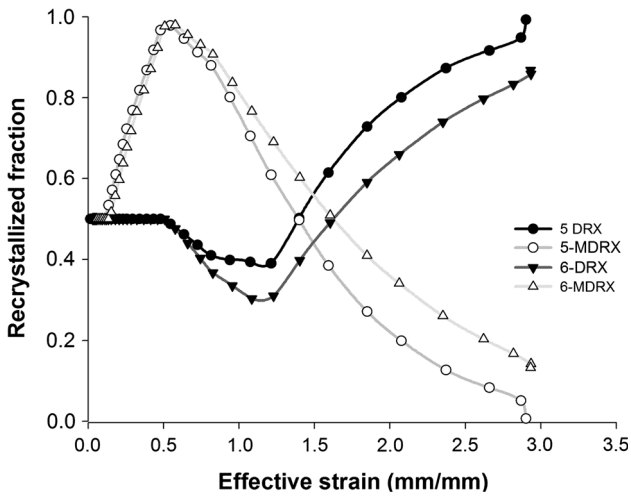


**Fig. 7** Numerical results of effective strain vs. dynamic and metadynamic recrystallized fraction

different grains morphological changes. Considering the previous aspects, one possibility to decrease divergence in the Avrami models applied could be through experimental evaluation of recrystallization kinetics at low strains and temperatures higher than δ solvus.

## 6. Conclusions

Recrystallization and grain size evolution was observed through experimental hot die forging trials. Finite element data and phenomenological models were used to predict microstructure changes occurring after forging at temperature interval of 1253 to 1323 K.

- Different grain size distributions were observed in the forged specimens. Regions in contact with operation tools showed localized flow and limited deformation, in contrast to the regions located near the central zone of specimens

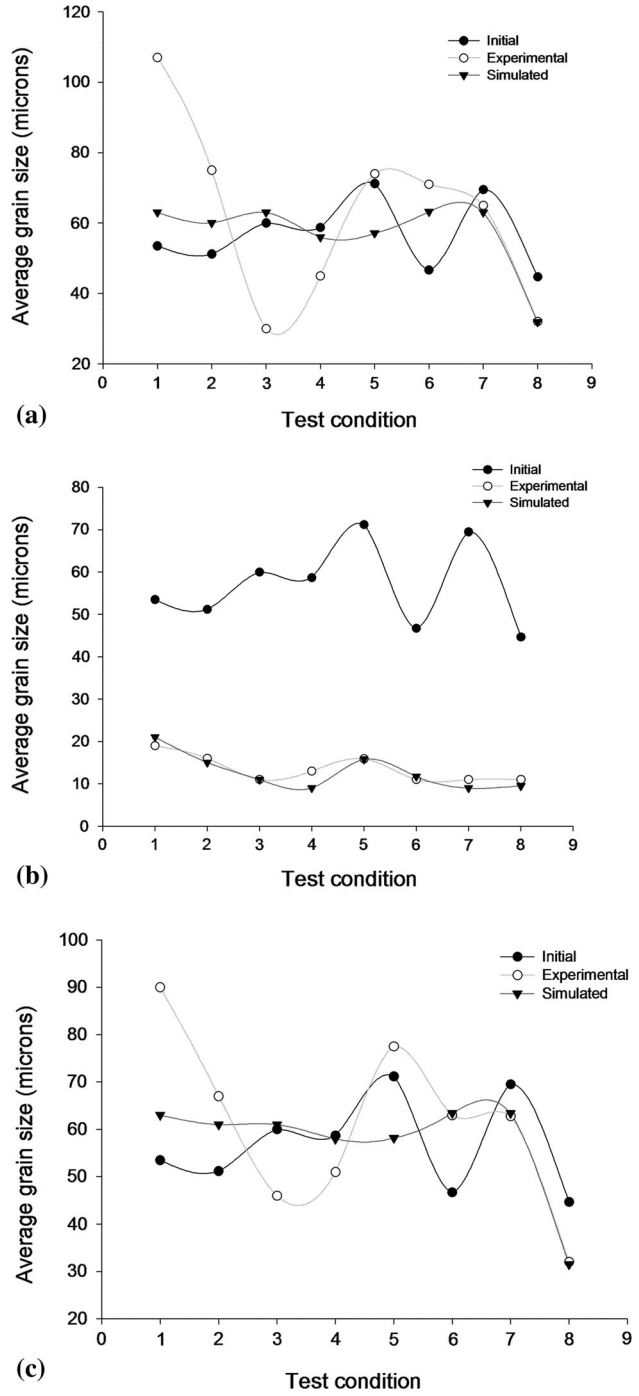


**Fig. 8** Experimental and numerical results of average grain size vs. forging condition. (a) Top, (b) center, and (c) bottom zone

where a greater deformation and a full recrystallized fraction were observed. In this last region, a good fit was obtained with simulated results.

- Specimens forged at two stages between 1273 and 1253 K showed a fully refined microstructure. Numerical model presents good fit with experimental results. In these forging sequences, the second deformation produces a secondary recrystallization resulting in a smaller grain. The grain size and recrystallized fraction of the forged specimens have a great dependence on forging characteristics and location of evaluation.

## Acknowledgments

The authors acknowledge the financial support provided by the Consejo Nacional de Ciencia y Tecnología CONACYT, Mexico. A special recognition goes to FRISA Forjados S.A. de C.V. for the facilities for carrying out this project.

## References

1. J.R. Davis, *ASM Specialty Handbook: Nickel, Cobalt, and Their Alloys*, ASM International, Materials Park, 2000
2. P.J. Páramo Kañetas, L.A. Reyes Osorio, M.P. Guerrero Mata, M. De La Garza, V. Páramo López, Influence of the Delta Phase in the Microstructure of the Inconel 718 subjected to "Delta-processing" Heat Treatment and Hot Deformed, *International Congress of Science and Technology of Metallurgy and Materials, SAM - CONAMET 2013, Procedia Materials Science*, Vol 8, 2015, p 1160–1165
3. L. Chamanfar, S.M. Jahazi, M. Asadi, A. Weck, and A.K. Koul, Microstructural Characteristics of Forged and Heat Treated Inconel-718 Disks, *Mater. Des.*, 2013, **52**, p 791–800
4. S.-H. Zhang, H.-Y. Zhang, and M. Cheng, Tensile Deformation and Fracture Characteristics of Delta-Processed Inconel 718 Alloy at Elevated Temperature, *Mater. Sci. Eng. A*, 2011, **528**(19–20), p 6253–6258
5. A. Niang, B. Viguier, and J. Lacaze, Some features of anisothermal solid-state transformations in alloy 718, *Mater Charact*, 2010, **61**(5), p 525–534
6. J. De Jaeger, D. Solas, T. Baudin, O. Fandeur, J.-H.Schmitt, et al. Inconel 718 Single and Multipass Modelling of Hot Forging. E.S. Huron, R.C. Reed, M.C. Hardy, M.J. Mills, R.E. montero, P.D. Portella, J.Telesman, Ed., John Wiley & Sons Inc., p 663–672, 2012, Superalloys 2012, TMS (The Minera, metal& material society)
7. L.A. Reyes, P. Páramo, A. Salas Zamarripa, M. de la Garza, and M.P. Guerrero Mata, Grain Size Modeling of a Ni-Base Superalloy Using Cellular Autómata Algorithm, *Mater. Des.*, 2015, **83**, p 301–307
8. T. Sakai, A. Belyakov, R. Kaibyshev, H. Miura, and J.J. Jonas, Dynamic and Post-dynamic Recrystallization Under Hot, Cold and Severe Plastic Deformation Conditions, *Prog. Mater Sci.*, 2014, **60**, p 130–207
9. J.P. Thomas, F. Montheillet, S.L. Semiatin, Modeling of Microstructure Evolution During the Thermo-Mechanical Processing of Nickel-Base Superalloys, ASM Handbook 22A (2009) 566–582
10. M. Tisza, Z. Lukács, and G. Gál, Numerical Modelling of Hot Forming Processes, *Int. J. Microstruct. Mater. Prop.*, 2008, **3**(1), p 21–34
11. X.-M. Chen, Y.C. Lin, D.-X. Wen, J.-L. Zhang, and M. He, Dynamic Recrystallization Behavior of a Typical Nickel-Based Superalloy During Hot Deformation, *Mater. Des.*, 2014, **57**, p 568–577
12. Y.C. Lin, D.-X. Wen, J. Deng, G. Liu, and J. Chen, Constitutive Models for High-temperature flow Behaviors of a Ni-Based Superalloy, *Mater. Des.*, 2014, **59**, p 115–123
13. Y.C. Lin, J. Deng, Y.Q. Jiang, D.X. Wen, and G. Liu, Hot Tensile Deformation and Fracture Characteristics of a Typical Ni-Based Superalloy at Elevated Temperature, *Mater. Des.*, 2014, **55**, p 949–957
14. Y.C. Lin, X.-M. Chen, D.-X. Wen, and M.-S. Chen, A Physically-Based Constitutive Model for a Typical Nickel-Based Superalloy, *Comput. Mater. Sci.*, 2014, **83**(15), p 282–289
15. D. Christian and G. Eric, Microstructure Prediction During Incremental Processes for Hot Forming of 718 Alloy, *Adv. Mater. Res.*, 2011, **278**, p 186–191
16. Andrea Agnoli, Marc Bernacki, Roland Logé, Jean-Michel Franchet, Johanne Laigo, and Nathalie Bozzolo, Selective Growth of Low Stored Energy Grains During d Sub-solvus Annealing in the Inconel 718 Nickel-Based Superalloy, *Metall. Mater. Trans. A*, 2011, **46A**, p 4405–4421
17. H.W. Lee, S.H. Kang, and Y.S. Lee, Prediction of Microstructure Evolution during Hot Forging Using Grain Aggregate Model for Dynamic Recrystallization, *Int. J. Precis. Eng. Manuf.*, 2014, **15**(6), p 1055–1062
18. C. Bos, M.G. Mecozzi, and J. Sietsma, A Microstructure Model for Recrystallisation and Phase Transformation During the Dual-Phase Steel Annealing Cycle, *Comput. Mater. Sci.*, 2010, **48**, p 692–699

19. Y.C. Lin and Wu Xian-Yang, A New Method for Controlling Billet Temperature During Isothermal Die Forging of a Complex Superalloy Casing, *J. Mater. Eng. Perform.*, 2015, **24**(9), p 3549–3557
20. "Standard Test Methods for Determining Average Grain Size" ASTM E112-13, ASTM, 2013
21. J.M. Zhang, Z.Y. Gao, J.Y. Zhuang, and Z.Y. Zhong, Grain Growth Model of IN718 During Holding Period After Hot Deformation, *J. Mater. Process. Technol.*, 2000, **101**(1-3), p 25–30
22. S.C. Medeiros, Y.V.R.K. Prasad, W.G. Frazier, and R. Srinivasan, Microstructural Modeling of Metadynamic Recrystallization in Hot Working of IN 718 Superalloy, *Mater. Sci. Eng. A*, 2000, **293**, p 198–207
23. M. Tisza, Z. Lukács, and G. Gál, Numerical Modelling of Hot Forming Processes, *Int. J. Microstruct. Mater. Prop.*, 2008, **3**(1), p 21–34
24. R. Srinivasan, V. Ramnarayan, U. Deshpande, V. Jain, and I. Weiss, Computer Simulation of the Forging of Fine Grain IN-718 Alloy, *Metall. Mater. Trans. A*, 1993, **24A**, p 2061
25. J.-L. Chenot, Advanced Numerical methods for F. E. Simulation of Metal Forming Processes, *Proceedings of the 10th International Conference on Numerical Methods in Industrial Forming Processes, AIP Conference Proceedings*, 2010, 1252, p 27–38
26. X.-M. Chen, Y.C. Lin, D.-X. Wen, J.-L. Zhang, and H. Min, Dynamic Recrystallization Behavior of a Typical Nickel-Based Superalloy During Hot Deformation, *Mater. Design*, 2014, **57**, p 568–577
27. D. Huang, W.T. Wu, D. Lambert, S.L. Semiatin, Computer Simulation of Microstructure Evolution During Hot Forging of Waspaloy and Nickel Alloy 718, *Proceedings of Microstructure Modeling and Prediction During Thermomechanical Processing,* R. Srinivasan, S.L. Semiatin, A. Beaudoin, S. Fox, Z. Jin, Eds., TMS, 2001, p 137–46
28. L.X. Zhou and T.N. Baker, Effects of Dynamic and Metadynamic Recrystallization on Microstructures of Wrought IN 718 Due to Hot Deformation, *Mater. Sci. Eng. A.*, 1995, **196**, p 89–95
29. F. Montheillet, Models of Recrystallization, ASM Handbook, Vol 22A: Fundamentals of Modeling for Metals Processing, ASM International, 2009
30. S. Coste, Thèse "Determination des Lois D'évolution Microstructurale de L'alliage 718 Lors du Matriçage," ENSIACET, 2003, (in French)
31. J. Uginet, J. Jackson, Alloy 718 Forging Development for Large Land-Based Gas Turbines, Superalloys 718, 625, 706 and Derivatives, TMS, 2005, p 57-67
32. N.-K. Park, J.-T. Yeom, Y.-S. Na, I.S. Kim, D.H. Kim, S.J. Choe, Two step forging of Alloy 718, *Proceedings of the International Symposium on Superalloys* 718, 625, 706 and Various Derivatives, June 15–18, Pittsburgh, USA, TMS, 1997, p 173–82